Threshold Setting for Adaptive Matched Filter and Adaptive Coherence Estimator

Jun Liu, *Member, IEEE*, Hongbin Li, *Senior Member, IEEE*, and Braham Himed, *Fellow, IEEE*

***Abstract*—It is known that the probabilities of false alarm (PFAs) of several celebrated adaptive detectors including the adaptive matched filter (AMF) and the adaptive coherence estimator (ACE) can be expressed as integral forms. Nevertheless, it is inconvenient to set the detection thresholds by using these integral expressions. Here, we propose two computationally efficient schemes to calculate the thresholds of the AMF and ACE. In the first method, approximate expressions, in forms of elementary functions, for the PFAs of the AMF and ACE are derived. The thresholds of the AMF and ACE can be numerically computed by using these elementary expressions instead of the integrals, for reducing computational complexity. In the second approach, further approximations are employed to lead to highly simple expressions for the thresholds of the AMF and ACE, which enable us to directly compute the thresholds for a given PFA. Compared to the first one, the second scheme is more computationally efficient, but at the cost of a slight loss in accuracy. Numerical results verify the effectiveness of the two proposed schemes.**

***Index Terms*—Adaptive coherence estimator, adaptive detection, adaptive matched filter, generalized likelihood ratio test, Laplace approximation, Rao test.**

I. Introduction

DETECTING a signal of interest (SOI) in Gaussian noise with an unknown covariance matrix is a common problem in space-time adaptive processing (STAP) [1]–[3]. Typically, the presence of SOI is sought in a (range) cell under test (CUT), based on a single observation or multiple observations which are referred to as test data (primary data). To this end, a set of training data (secondary data) samples, which contain noise only, are employed to estimate the unknown noise covariance matrix. In radar, these training data samples are usually collected from range cells adjacent to the CUT.

Manuscript received April 02, 2014; accepted July 29, 2014. Date of publication August 11, 2014; date of current version August 13, 2014. This work was supported in part by a subcontract with Dynetics, Inc. for research sponsored by the Air Force Research Laboratory (AFRL) under Contract FA8650-08-D-1303. The associate editor coordinating the review of this manuscript and approving it for publication was Dr. Keith Davidson.

J. Liu was with the Department of Electrical and Computer Engineering, Stevens Institute of Technology, Hoboken, NJ 07030 USA. He is now with the National Laboratory of Radar Signal Processing, Xidian University, Xi'an 710071, China (e-mail: jun_liu_math@hotmail.com).

H. Li is with the Department of Electrical and Computer Engineering, Stevens Institute of Technology, Hoboken, NJ 07030 USA (e-mail: hongbin.li@stevens.edu).

B. Himed is with AFRL/RYMD, Dayton, OH 45433 USA (e-mail: braham.himed@wpafb.af.mil).

Color versions of one or more of the figures in this paper are available online at http://ieeexplore.ieee.org.

Digital Object Identifier 10.1109/LSP.2014.2345757

In an ideal situation, the noise in the training data is assumed to share the same covariance matrix as that in the test data. This situation is often referred to as a homogeneous environment. In this case, many classic detectors have been proposed. More specifically, a generalized likelihood ratio test (GLRT) was first proposed by Kelly in [4]. Then, Robey *et al.*, derived an adaptive matched filter (AMF) by using a two-step procedure [5]. Interestingly, it is proved in [6] that the Wald test coincides with the AMF. In addition, De Maio develops a Rao test in [7]. Each test mentioned above has a constant false alarm rate property with respect to the unknown noise covariance. In particular, simple expressions for the probabilities of false alarm (PFAs) of the GLRT and Rao test have been obtained in [4] and [6], respectively. As a result, the detection threshold of the GLRT or Rao test can be expressed as an elementary function with respect to the PFA, which enables us to directly compute the threshold for any given PFA. However, the PFA of the AMF is obtained as an integral form [5], [8], which cannot be used to directly calculate the detection threshold. Hence, numerical techniques, although time-consuming, have to be employed to find the threshold of the AMF for a given PFA.

In practice, partially homogeneous environments may be encountered, where the noise covariance matrix has the same structure in the test and training data samples but may differ by a scaling factor [9], [10]. To address the detection problem in partially homogeneous environments, an adaptive coherence estimator (ACE) was proposed in [9], [11]. It is proved in [12], [13] that in the partially homogeneous case, both the Rao and Wald tests exhibit the same form as the ACE test. In [14], the PFA of the ACE test is derived in terms of an integral. Nevertheless, we cannot directly calculate the threshold for a given PFA by using the integral whose invertibility with respect to the threshold does not exist analytically. Thus, numerical techniques have to be used to obtain the threshold in the ACE, as in the AMF.

In this study, our main contribution is to propose two computationally efficient approaches for the threshold setting of the AMF and ACE. In the first method, the PFAs of the AMF and ACE are approximated by elementary functions which can be used to numerically calculate the thresholds with less computational complexity. In the second method, an approximate but impressively simple expression for the thresholds of the AMF and ACE are derived, which can be used to directly design the thresholds of the AMF and ACE, as in the GLRT and Rao test. Simulation results show that the thresholds obtained with these approximate expressions match the thresholds obtained via Monte Carlo (MC) techniques. The second scheme has a

less computational burden than the first one, but at the expense of an insignificant loss in accuracy.

II. Problem Formulation

Consider the data model widely used in STAP [1]:

$$\mathbf{x} = \mathbf{s}a + \mathbf{n}, \tag{1}$$

where $\mathbf{s}$ is a known steering vector of dimension $Q \times 1$; a is a deterministic but unknown complex scalar accounting for the target reflectivity and the channel propagation effects; the noise $\mathbf{n}$ is assumed to have a circularly symmetric, complex Gaussian distribution, i.e., $\mathbf{n} \sim \mathcal{CN}(\mathbf{0}, \alpha\mathbf{R})$, where α is a scaling of the noise in the test data, and $\mathbf{R}$ is a positive definite covariance matrix of dimension $Q \times Q$.

In practice, the noise covariance matrix structure $\mathbf{R}$ is usually unknown. To estimate $\mathbf{R}$, one often imposes a standard assumption that there exists a set of training data (secondary data) free of target signal components, i.e., $\{\mathbf{y}_k | \mathbf{y}_k \sim \mathcal{CN}(\mathbf{0}, \mathbf{R}), k = 1, 2, \ldots, K \text{ and } K \geq Q\}$. Note that the scaling factor α accounts for the non-homogeneity between the test and training data. In particular, $\alpha = 1$ and $\alpha \neq 1$ correspond to homogeneous and partially homogeneous environments, respectively [15].

A. AMF

In the homogeneous case where $\alpha = 1$, the AMF is proposed as [5]

$$\Lambda_{\mathrm{AMF}} = \frac{|\mathbf{s}^\dagger \hat{\mathbf{R}}^{-1}\mathbf{x}|^2}{\mathbf{s}^\dagger \hat{\mathbf{R}}^{-1}\mathbf{s}} \underset{\mathcal{H}_0}{\overset{\mathcal{H}_1}{\gtrless}} \lambda_{\mathrm{AMF}}, \tag{2}$$

where $\mathcal{H}_1$ and $\mathcal{H}_0$ are the target-present and target-absent hypotheses, respectively; $(\cdot)^\dagger$ denotes complex conjugate transpose; $|\cdot|$ is the modulus of a complex number; λ_{AMF} is the corresponding detection threshold, and $\hat{\mathbf{R}} = \sum_{k=1}^{K} \mathbf{y}_k \mathbf{y}_k^\dagger$.

The PFA of the AMF is given in an integral form [5], [8], i.e.,

$$P_{\mathrm{FA}}^{\mathrm{AMF}} = \int_0^1 P_{\mathrm{FA}|\rho}^{\mathrm{AMF}} f(\rho) \mathrm{d}\rho, \tag{3}$$

where

$$f(\rho) = \frac{K!}{(Q-2)!(K-Q+1)!}(1-\rho)^{Q-2}\rho^{K-Q+1}, \tag{4}$$

and

$$P_{\mathrm{FA}|\rho}^{\mathrm{AMF}} = (1 + \rho\lambda_{\mathrm{AMF}})^{-(K-Q+1)}. \tag{5}$$

Obviously, it is not easy to compute the invertibility of the integral expression (3) with respect to λ_{AMF}.

B. ACE

For the partially homogeneous case where $\alpha \neq 1$, the ACE is proposed as [11], [9]

$$\Lambda_{\mathrm{ACE}} = \frac{|\mathbf{s}^\dagger \hat{\mathbf{R}}^{-1}\mathbf{x}|^2}{(\mathbf{s}^\dagger \hat{\mathbf{R}}^{-1}\mathbf{s})(\mathbf{x}^\dagger \hat{\mathbf{R}}^{-1}\mathbf{x})} \underset{\mathcal{H}_0}{\overset{\mathcal{H}_1}{\gtrless}} \lambda_{\mathrm{ACE}}, \tag{6}$$

where λ_{ACE} is the detection threshold. As derived in [14], the PFA of the ACE is

$$P_{\mathrm{FA}}^{\mathrm{ACE}} = \int_0^1 P_{\mathrm{FA}|\rho}^{\mathrm{ACE}} f(\rho) \mathrm{d}\rho, \tag{7}$$

where $f(\rho)$ is defined in (4), and

$$P_{\mathrm{FA}|\rho}^{\mathrm{ACE}} = \left(\frac{1-\lambda_{\mathrm{ACE}}}{1-\rho\lambda_{\mathrm{ACE}}}\right)^{K-Q+1}. \tag{8}$$

Obviously, it is inconvenient to use the integral expression (7) to set the detection threshold.

The statements above indicate that the detection thresholds of the AMF and ACE cannot be computed in a simple way similar to that in the GLRT [4] and Rao test [7]. To circumvent this drawback, we derive approximate but elementary expressions for the PFAs of the AMF and ACE, by using the Laplace approximation method in [16].

III. Threshold Computation

A. Threshold Setting for AMF

The PFA of the AMF in (3) can be rewritten as

$$\begin{aligned} P_{\mathrm{FA}}^{\mathrm{AMF}} &= \frac{K!}{(Q-2)!(K-Q+1)!} \\ &\quad \times \int_0^1 \rho^{K-Q+1}(1-\rho)^{Q-2}(1+\rho\lambda_{\mathrm{AMF}})^{-(K-Q+1)}\mathrm{d}\rho \\ &= {}_2F_1(K-Q+1, K-Q+2; K+1; -\lambda_{\mathrm{AMF}}), \end{aligned} \tag{9}$$

where the second equation is obtained by [17, p. 317, eq. (3.197.3)], and ${}_2F_1(a, b; c; x)$ is the Gaussian hypergeometric function defined as [17]

$${}_2F_1(a, b; c; x) = \sum_{k=0}^{\infty} \frac{(a)_k (b)_k}{(c)_k k!} x^k \tag{10}$$

with $(n)_k = n(n+1)\cdots(n+k-1)$ being the Pochhammer symbol.

According to [16, eq. 24], the Gaussian hypergeometric function can be approximated by

$$P_{\mathrm{FA}}^{\mathrm{AMF}} \approx G(K-Q+1, K-Q+2; K+1; -\lambda_{\mathrm{AMF}}), \tag{11}$$

where $G(a, b; c; x)$ is an *elementary* function defined in (A.1) of Appendix A. As shown in Appendix A, for $\lambda_{\mathrm{AMF}} \to 0$, we obtain

$$P_{\mathrm{FA}}^{\mathrm{AMF}} \approx \left(1 + \frac{K-Q+1}{K+1}\lambda_{\mathrm{AMF}}\right)^{-(K-Q+2)}. \tag{12}$$

Hence, the approximate threshold of the AMF is

$$\lambda_{\mathrm{AMF}} \approx \frac{K+1}{K-Q+1}\left[\left(P_{\mathrm{FA}}^{\mathrm{AMF}}\right)^{-\frac{1}{K-Q+2}} - 1\right]. \tag{13}$$

B. Threshold Setting for ACE

The PFA of the ACE in (7) can be rewritten as

$$P_{\mathrm{FA}}^{\mathrm{ACE}} = \frac{K!(1-\lambda_{\mathrm{ACE}})^{K-Q+1}}{(Q-2)!(K-Q+1)!}$$

$$\times \int_0^1 \rho^{K-Q+1}(1-\rho)^{Q-2}(1-\rho\lambda_{\mathrm{ACE}})^{-(K-Q+1)}\mathrm{d}\rho$$
$$= (1-\lambda_{\mathrm{ACE}})^{K-Q+1} \times {}_2F_1(K-Q+1, K-Q+2; K+1; \lambda_{\mathrm{ACE}}). \quad (14)$$

Due to [16, eq. 24], we have

$$P_{\mathrm{FA}}^{\mathrm{ACE}} \approx (1-\lambda_{\mathrm{ACE}})^{K-Q+1} G(K-Q+1, K-Q+2; K+1; \lambda_{\mathrm{ACE}}), \quad (15)$$

where $G(a,b;c;x)$ is defined in (A.1). For $\lambda_{\mathrm{ACE}} \to 0$, we further have

$$P_{\mathrm{FA}}^{\mathrm{ACE}} \approx (1-\lambda_{\mathrm{ACE}})^{K-Q+1}\left(1-\frac{K-Q+1}{K+1}\lambda_{\mathrm{ACE}}\right)^{-(K-Q+2)} \approx \left(\frac{1-\lambda_{\mathrm{ACE}}}{1-\frac{K-Q+1}{K+1}\lambda_{\mathrm{ACE}}}\right)^{K-Q+1}, \quad (16)$$

where the first equation is derived with (A.8), and the second equation is obtained with the fact that when $\lambda_{\mathrm{ACE}} \to 0$,

$$1-\frac{K-Q+1}{K+1}\lambda_{\mathrm{ACE}} \to 1. \quad (17)$$

It follows from (16) that the approximate threshold of the ACE is

$$\lambda_{\mathrm{ACE}} \approx \frac{1-\left(P_{\mathrm{FA}}^{\mathrm{ACE}}\right)^{\frac{1}{K-Q+1}}}{1-\frac{K-Q+1}{K+1}\left(P_{\mathrm{FA}}^{\mathrm{ACE}}\right)^{\frac{1}{K-Q+1}}}. \quad (18)$$

It should be emphasized that the expressions in (13) and (18) for the detection thresholds are very simple functions with respect to the PFA. Thus, the detection threshold of the AMF or ACE can be directly computed for a given PFA. The approximation accuracy of (13) and (18) will be demonstrated in the next section.

IV. Simulation Results

In this section, numerical simulations are conducted to check the validity of the above theoretical results. We consider a STAP system with 4 antennas and 10 coherent pulses, i.e., $Q = 40$. The (i,j)th element of the noise covariance matrix is chosen to be $[\mathbf{R}]_{i,j} = \sigma^2 0.9^{|i-j|}$, where σ^2 represents the noise power and is set to be 1.

In Fig. 1, the PFA of the AMF versus the detection threshold is presented for different values of K. The line, the symbols "$\circ$", and "$+$" denote the results obtained with (3), (11), and (12), respectively. It can be seen that the approximate results obtained with (11) match the exact ones obtained with (3) pretty well. It means that without sacrificing accuracy, the computational complexity can be significantly reduced by using the elementary expression in (11) instead of the integral in (3). In addition, there is a little loss in the accuracy of (12) compared to (11), mainly due to its two-step approximation.

The detection threshold of the AMF as a function of the training data size K is reported in Fig. 2. The line and the symbol "$+$" denote the results obtained by the MC simulation and (13), respectively. The number of independent trials used

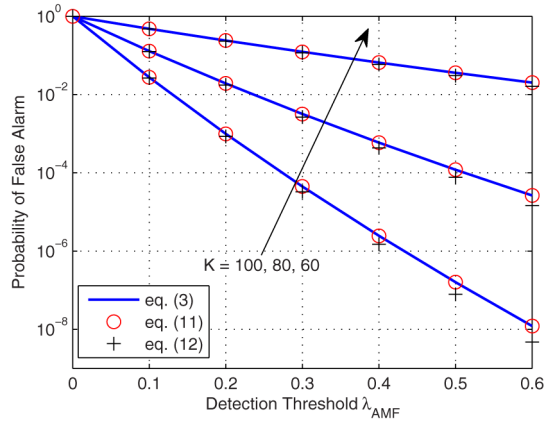

Fig. 1. Probability of false alarm of AMF with different K.

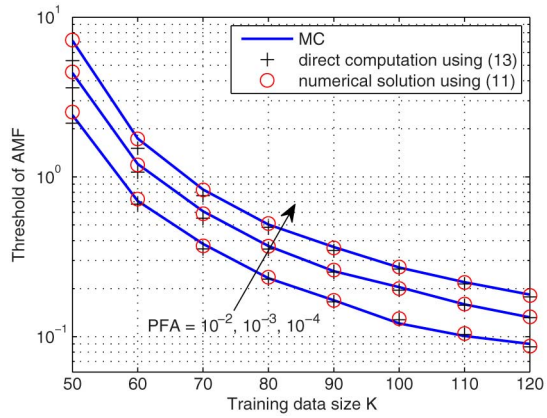

Fig. 2. Detection threshold of AMF versus K.

in each case is $100/P_{\mathrm{FA}}^{\mathrm{AMF}}$. We can observe that the thresholds calculated with the simple expression (13) are close to those obtained with MC simulations. However, the error is relatively large in some cases (e.g., $K = 50$ in this example). If high precision is required, caution must be taken when using (13) to compute the threshold of the AMF.

For obtaining highly accurate thresholds, we can use (11), instead of the integral expression (3), to numerically search for the threshold. Apparently, the computational burden is relieved due to avoiding the calculation of the integral. Note that the choice of an initialization value plays an important role in the numerical search. The approximate result obtained with (13), even though inexact, can be used as a good initialization in the numerical search. In Fig. 2, the symbol "$\circ$" denotes the result obtained by using (11) to numerically search for the threshold, where the approximate result obtained with (13) serves as the initialization. It can be seen that the thresholds by this numerical method are in very good agreement with the MC results.

In practical applications, we suggest (13) to calculate the threshold of the AMF due to its simplicity, if high accuracy in the threshold is not required. When a precise threshold is needed, (11) is preferred since it avoids the computation of the integral or hypergeometric function, without sacrificing the accuracy.

Fig. 3 depicts the PFA of the ACE as a function of detection threshold for different values of K. The line, the symbols "$\circ$", and "$+$" denote the results obtained with (7), (15), and (16),

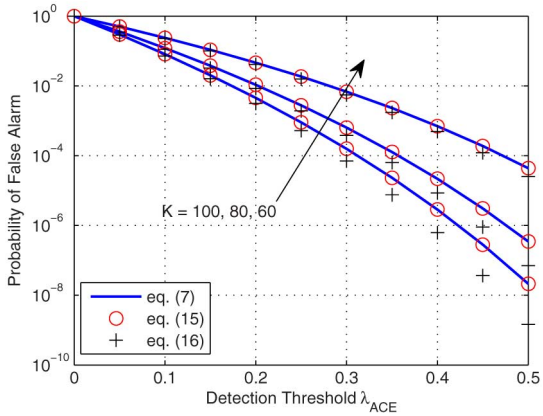

Fig. 3. Probability of false alarm of ACE with different K.

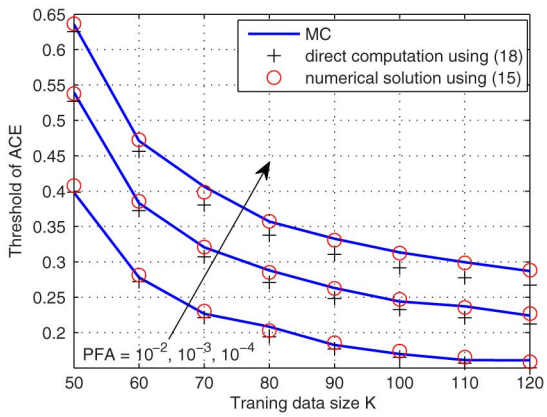

Fig. 4. Detection threshold of ACE versus K.

respectively. It is shown that the approximation accuracy of (15) and (16) is acceptable. Nevertheless, the error in (16) compared to (15) is large, due to the three-step approximation in deriving (16).

Fig. 4 compares the thresholds obtained by (15), (18), and the MC simulations. When employing (15) to numerically compute the threshold, we use the results obtained with (18) as initialization. It is shown that the thresholds obtained using (15) and (18) are close to the MC simulations. Additionally, the accuracy of (15) compared to (18) is higher, but at the expense of more computational burden. Nevertheless, the complexity in numerically searching for the threshold is significantly reduced by using (15) instead of (7).

Therefore, (15) is recommended if a high accuracy in the threshold of the ACE is required in practice. Otherwise, (18) is suggested due to its simplicity.

V. Conclusion

In the existing literature, the PFA of the AMF (or ACE) is expressed in terms of an integral or Gaussian hypergeometric function. Obviously, it is inconvenient to set the detection threshold by using the integral or Gaussian hypergeometric expression. To overcome it, two approximate schemes are proposed. In the first scheme, highly accurate but elementary expressions for the PFAs of the AMF and ACE are given. The computational complexity in numerically searching for the threshold is significantly reduced without sacrificing accuracy by using these elementary expressions compared to the integrals or Gaussian hypergeometric expressions. In the second scheme, the thresholds of the AMF and ACE are derived as approximate but very simple functions with respect to the PFA. These provide a simple and direct way to compute the thresholds for a preassigned PFA. Simulation results demonstrate that the approximation accuracy in the first scheme is better than that in the second scheme, but at a relatively higher computational cost. If high precision in the threshold is not needed, the second scheme is suggested. Otherwise, the first one is recommended.

Appendix A

According to [16, eq. 24], given positive numbers a, b, and c and any real number x, we can approximate ${}_2F_1(a,b;c;x)$ by $G(a,b;c;x)$ which is defined as

$$G(a,b;c;x) = c^{c-\frac{1}{2}} r^{-\frac{1}{2}} \left(\frac{y}{a}\right)^a \left(\frac{1-y}{c-a}\right)^{c-a} (1-xy)^{-b}, \tag{A.1}$$

where

$$y = \frac{2a}{\sqrt{\tau^2 - 4ax(c-b)} - \tau}, \tag{A.2}$$

and

$$r = \frac{y^2}{a} + \frac{(1-y)^2}{c-a} - \frac{b}{a(c-a)} L^2 \tag{A.3}$$

with

$$\tau = x(b-a) - c, \tag{A.4}$$

and

$$L = \frac{xy(1-y)}{1-xy}. \tag{A.5}$$

When $x \to 0$, we have

$$\tau \to -c, \text{ and } L \to 0. \tag{A.6}$$

Then,

$$y \to \frac{a}{c}, \text{ and } r \to \frac{1}{c}. \tag{A.7}$$

Inserting (A.7) into (A.1) results in

$${}_2F_1(a,b;c;x) \approx G(a,b;c;x) \approx \left(1 - \frac{a}{c}x\right)^{-b}. \tag{A.8}$$

References

[1] J. Ward, Space-time adaptive processing for airborne radar Lincoln Laboratory, MIT, Tech. Rep. 1015, Dec. 1994.

[2] W. Liu, W. Xie, J. Liu, and Y. Wang, "Adaptive double subspace signal detection in Gaussian background–Part I: Homogeneous environments," *IEEE Trans. Signal Process.*, vol. 62, no. 9, pp. 2345–2357, May 2014.

[3] W. Liu, W. Xie, J. Liu, and Y. Wang, "Adaptive double subspace signal detection in Gaussian background–Part II: Partially homogeneous environments," *IEEE Trans. Signal Process.*, vol. 62, no. 9, pp. 2358–2369, May 2014.

[4] E. J. Kelly, "An adaptive detection algorithm," *IEEE Trans. Aerosp. Electron. Syst.*, vol. AES-22, no. 1, pp. 115–127, Mar. 1986.

[5] F. C. Robey, D. R. Fuhrmann, E. J. Kelly, and R. Nitzberg, "A CFAR adaptive matched filter detector," *IEEE Trans. Aerosp. Electron. Syst.*, vol. 28, no. 1, pp. 208–216, Jan. 1992.

[6] A. De Maio, "A new derivation of the adaptive matched filter," *IEEE Signal Process. Lett.*, vol. 11, no. 10, pp. 792–793, Oct. 2004.

[7] A. De Maio, "Rao test for adaptive detection in Gaussian interference with unknown covariance matrix," *IEEE Trans. Signal Process.*, vol. 55, no. 7, pp. 3577–3584, Jul. 2007.

[8] J. Liu, Z.-J. Zhang, and Y. Yun, "Optimal waveform design for generalized likelihood ratio and adaptive matched filter detectors using a diversely polarized antenna," *Signal Process.*, vol. 92, no. 4, pp. 1126–1131, Apr. 2012.

[9] S. Kraut, L. L. Scharf, and R. W. Butler, "The adaptive coherence estimator: A uniformly-most-powerful-invariant adaptive detection statistic," *IEEE Trans. Signal Process.*, vol. 53, no. 2, pp. 417–438, Feb. 2005.

[10] J. Liu, Z.-J. Zhang, and Y. Yang, "Performance enhancement of subspace detection with a diversely polarized antenna," *IEEE Signal Process. Lett.*, vol. 19, no. 1, pp. 4–7, Jan. 2012.

[11] E. Conte, M. Lops, and G. Ricci, "Asymptotically optimum radar detection in compound Gaussian clutter," *IEEE Trans. Aerosp. Electron. Syst.*, vol. 31, no. 2, pp. 617–625, Apr. 1995.

[12] A. De Maio and S. Iommelli, "Coincidence of the Rao test, Wald test, and GLRT in partially homogeneous environment," *IEEE Signal Processing Lett.*, vol. 15, no. 4, pp. 385–388, Apr. 2008.

[13] W. Liu, Y. Wang, and W. Xie, "Fisher information matrix, Rao test, and Wald test for complex-valued signals and their applications," *Signal Process.*, vol. 94, no. 1, pp. 1–5, Jan. 2014.

[14] J. Liu, Z.-J. Zhang, Y. Yang, and H. Liu, "A CFAR adaptive subspace detector for first-order or second-order Gaussian signals based on a single observation," *IEEE Trans. Signal Process.*, vol. 59, no. 11, pp. 5126–5140, Nov. 2011.

[15] J. Liu, Z.-J. Zhang, P.-L. Shui, and H. Liu, "Exact performance analysis of an adaptive subspace detector," *IEEE Trans. Signal Process.*, vol. 60, no. 9, pp. 4945–4950, Sep. 2012.

[16] R. W. Butler and A. T. A. Wood, "Laplace approximations for hypergeometric functions with matrix argument," *Ann. Statist.*, vol. 30, no. 4, pp. 1155–1177, Aug. 2002.

[17] I. S. Gradshteyn and I. M. Ryzhik*, Table of Integrals, Series, and Products*, 7th Ed. ed. San Diego, CA, USA: Academic, 2007.